A TWO-DIMENSIONAL TRAJECTORY-SIMULATION MODEL FOR NON-GAUSSIAN, INHOMOGENEOUS TURBULENCE WITHIN PLANT CANOPIES

T. K. FLESCH and J. D. WILSON

Division of Meteorology, Department of Geography, University of Alberta, Edmonton, Alberta, Canada T6G 2H4

(Received in final form, 23 April, 1992)

Abstract. We report a two-dimensional (alongwind u, vertical w) trajectory-simulation model, consistent with Thomson's (1987) well-mixed criteria, that allows for the non-Gaussian turbulence typical of flow within a plant canopy. The effect of non-Gaussian turbulence was examined by formulating a non-Gaussian u, w joint probability density function (PDF) as the sum of two Gaussian joint-PDFs. The resultant PDF reproduced the desired means, variances, skewnesses, and kurtoses, and the correct covariance. In prediction of the location of maximum concentration downwind of a line source in homogeneous, slightly non-Gaussian turbulence, it proved advantageous to incorporate skewness and kurtosis. However, in the case of inhomogeneous, highly non-Gaussian turbulence, the addition of skewness and kurtosis in the model resulted in substantially worse agreement with measurements than the results of the model using Gaussian PDFs. This may be due to inaccuracy in our PDF formulation. Dispersion predictions from the model with Gaussian PDFs were generally not statistically different from measurements. These results indicate that a two-dimensional Gaussian trajectory-simulation approach is adequate to predict mean concentrations and fluxes resulting from sources within plant canopies.

1. Introduction

The turbulent dispersion of aerosols within and above plant canopies is important in many agricultural and biological problems. The spread of plant pathogens, the effectiveness of pesticide spray applications, and fertilizer and pesticide volatilization from the soil are examples of processes which are strongly influenced by turbulent dispersion. These and other problems have provided incentive for the development of dispersion models which can be used within plant canopies.

In general, Lagrangian methods provide the most natural approach to modelling turbulent dispersion. Their fundamental advantage when compared with Eulerian methods is the correct prediction of dispersion close to the source, in the "near-field" region (Raupach, 1989). In many problems a plant canopy or soil surface represents a spatially extensive source region, and correct treatment of near-field effects is especially important. The most powerful of Lagrangian methods in terms of versatility are trajectory-simulation models (also known as Monte Carlo or random flight models). These models numerically mimic the trajectories of marked fluid elements (particles) to create an ensemble average distribution of particle position and velocity. These distributions can then be used for example, to give the mean concentration downwind of a particle source. The computational basis of most trajectory-simulation models is a generalized Langevin equation, which

Boundary-Layer Meteorology **61**: 349–374, 1992.

follows from the assumption that particle position and velocity evolve as a Markov process. Consider a particle moving vertically in response to turbulence. If z and w are the vertical position and velocity of the particle respectively, then as a Markov process we may write a generalized Langevin equation for the change in particle velocity (Thompson, 1987):

$$\mathrm{d}w = a\,\mathrm{d}t + b\,\mathrm{d}\xi\,,$$

with the change in vertical position given as,

$$\mathrm{d}z = w\,\mathrm{d}t\,.$$

The coefficients a and b are to be determined, $\mathrm{d}t$ is the model time-step, and $\mathrm{d}\xi$ is a random velocity increment selected from a Gaussian distribution having mean 0 and variance $\mathrm{d}t$.

The first trajectory-simulation models were used to predict turbulent dispersion from continuous point sources well above any plant canopy (Thompson, 1971; Hall, 1975; Reid, 1979). They were (at best) suitable for an idealized atmosphere having Gaussian vertical turbulence. These models were quite simple due to the straightforward form of the Langevin equation in such an atmosphere, and produced surprisingly accurate results.

Predicting dispersion within a plant canopy represents a more challenging application for trajectory-simulation models. The grossly inhomogeneous nature of turbulence within a canopy is well documented. The turbulence is highly non-Gaussian as well. Vertical velocity distributions often show skewness ($\mathrm{Sk}_w = \overline{w^3}/\sigma_w^3$, where σ_w is the standard deviation of w) below -1 and kurtosis ($\mathrm{Kt}_w = \overline{w^4}/\sigma_w^4$) exceeding 10 (Baldocchi and Meyers, 1989; Amiro, 1990; Leclerc *et al.*, 1991): a substantial deviation from Gaussian values of $\mathrm{Sk} = 0.0$ and $\mathrm{Kt} = 3.0$. An additional complication for a canopy dispersion model is the role of streamwise velocity fluctuations (u). Above a plant canopy the effect of u on dispersion is small, due to the low horizontal turbulent intensity (Hall, 1975), and a one-dimensional (w) model is often sufficient. But within a canopy, where the horizontal turbulent intensity is large, an accurate treatment of streamwise dispersion is important (Legg, 1983; Legg *et al.*, 1986).

The last 15 years has seen a somewhat *ad hoc* progression from models of one-dimensional, homogeneous, Gaussian turbulence to those allowing for more complex flow. Wilson *et al.* (1981), Legg and Raupach (1982), and Leclerc *et al.* (1988) included, by differing methods, the effect of vertical inhomogeneity of σ_w (unless appropriate allowances are made, there is the incorrect tendency for particles to accumulate in the region where σ_w is small). Non-Gaussian turbulence was first included in the model of Legg (1983), who introduced Sk_w by selecting the Langevin random velocity increment from a skewed distribution. De Bass *et al.* (1986) and Sawford and Guest (1987) also used non-Gaussian random forcing to produce Sk_w. Although these models showed agreement with experimental results, it is now accepted that non-Gaussian random forcing in a Langevin equation is incorrect (Gardiner, 1983). The effect of streamwise turbulence was included in the models of Hall (1975), Hanna (1978), and Legg (1983). Hall (1975) added $\pm 2.2u_*$ to the mean horizontal velocity at each calculation, the sign being chosen to maintain the proper *u*-*w* covariance. Hanna (1978) included an independent Langevin equation for *u*, similar to that for *w*, with no *u*-*w* covariance. Legg (1983) used separate Langevin equations for *u* and *w* and included covariance by selecting a random velocity increment in the *u* equation which was correlated with the random increment in the *w* equation.

The development of trajectory-simulation models for complex turbulence had been hindered by the lack of definitive criteria for model formulation. But the efforts of Janicke (1983), Durbin (1983, 1984), Thomson (1984), and van Dop *et al.* (1985) to develop rigorous model criteria have culminated in the work of Thomson (1987) and his "well-mixed" criterion. Simply stated, this criterion requires that an initially well-mixed cloud of particles in an infinite domain should remain well-mixed. The importance of the well-mixed criterion is that it states the constraint implied by the Eulerian probability density functions (PDFs; presumed known) upon possible Lagrangian stochastic models. Consequently, the well-mixed criterion permits development of rigorously based trajectory-simulation models.

Luhar and Britter (1989) used the well-mixed criteria to develop a one-dimensional model for inhomogeneous, non-Gaussian turbulence in the convective boundary layer (CBL). They included Sk_w by using skewed PDFs which were created by summing two Gaussian distributions (Baerentsen and Berkowicz, 1984). Their results showed good agreement with laboratory experiments simulating dispersion in the CBL, and improved dispersion predictions over earlier models. A similar model was used by Weil (1990) and showed the importance of Sk_w in CBL dispersion. Neither of these models resolves a surface layer.

The objective of this study was to develop a two-dimensional (*u*, *w*) trajectory-simulation model which is consistent with the well-mixed criterion and applicable to the non-Gaussian inhomogeneous turbulence found within plant canopies. No two- or three-dimensional inhomogeneous, non-Gassian model has been derived to satisfy the well-mixed criterion. Two obstacles stand in the way of such a development. The first involves developing a Lagrangian stochastic model allowing non-Gaussian turbulence. In multi-dimensions the well-mixed criterion does not provide a unique model. This was demonstrated by Sawford and Guest (1988) who showed that two distinct Gaussian models, each satisfying the well-mixed criterion, gave slightly different results. At present there are no additional theoretical constraints to resolve this non-uniqueness. The second obstacle is the formulation of non-Gaussian velocity PDFs. Generalized multi-dimensional non-Gaussian PDFs are not commonly encountered in applied meteorology.

2. Trajectory-Simulation Model

2.1. Model development

The velocity of a fluid element (particle) in a horizontal (x) and vertical (z) plane was split into height-dependent, horizontally homogeneous mean horizontal velocity (U) and fluctuating turbulent velocities (u, w). Assuming that the particle's position and velocity evolve jointly as a Markov process, we specify a Langevin model for particle velocity and position:

$$\begin{aligned} \mathrm{d}u &= a_u\,\mathrm{d}t + b_u\,\mathrm{d}\xi_u\,, \\ \mathrm{d}x &= (u+U)\,\mathrm{d}t\,, \\ \mathrm{d}w &= a_w\,\mathrm{d}t + b_w\,\mathrm{d}\xi_w\,, \\ dz &= w\,\mathrm{d}t\,, \end{aligned} \tag{1}$$

where a_u, a_w, b_u, and b_w are generally functions of velocity and position, and $\mathrm{d}\xi_u$ and $\mathrm{d}\xi_w$ are independent random Gaussian increments with mean zero and variance $\mathrm{d}t$. The a_u and a_w are conditional mean values of the particle acceleration.

Consider a particle whose motion is governed by the above Markov process. Its state (x, z, u, w) evolves randomly in time, and can be represented as a point moving in four-dimensional phase space. The probability density $p(x, z, u, w, t)$ that the particle "occupies" a given position in the phase space evolves deterministically (from some initial value that relates to how the fluid element was chosen or released), and for the particular model (1) chosen here is governed by the Fokker–Planck equation:

$$\frac{\partial p}{\partial t} = -\frac{\partial(wp)}{\partial z} - \frac{\partial(a_u p)}{\partial u} - \frac{\partial(a_w p)}{\partial w} + \frac{1}{2}\frac{\partial^2(b_u p)}{\partial u^2} + \frac{1}{2}\frac{\partial^2(b_w p)}{\partial w^2}\,. \tag{2}$$

Of course, neither the Lagrangian stochastic model (1) nor the evolution of p according to Equation (2) is yet determined, for the a and b coefficients remain to be specified. Thomson's well-mixed criterion provides a constraint on these coefficients, namely that the Eulerian joint velocity PDF of all fluid elements at height z, $P_{uw}(z)$ (which we shall assume to be stationary), must be a solution of Equation (2). If we define,

$$a_u = \left[\phi_u + \frac{1}{2}\frac{\partial(b_u^2 P_{uw}(z))}{\partial u}\right]\Big/ P_{uw}(z)\,,$$

$$a_w = \left[\phi_w + \frac{1}{2}\frac{\partial(b_w^2 P_{uw}(z))}{\partial w}\right]\Big/ P_{uw}(z)\,,$$

then ϕ_u and ϕ_w can be considered a probability "current" in the u and w directions, and it is evident that $\phi_u/P_{uw}(z)$ and $\phi_w/P_{uw}(z)$ are effectively acceleration terms that "push" the increments in du and dw. Inserting a_u and a_w into Equation (2) gives:

$$\frac{\partial(wP_{uw}(z))}{\partial z} + \frac{\partial \phi_u}{\partial u} + \frac{\partial \phi_w}{\partial w} = 0 . \tag{3}$$

This is a continuity equation for probability in the u, w, z phase space. Conditions on ϕ_u and ϕ_w are (Thomson, 1987):

$$\phi_u, \phi_w \to 0 \qquad \text{as} \qquad |u, w| \to \infty . \tag{4}$$

The dilemma for any two- (or three-) dimensional model is the specification of ϕ_u and ϕ_w. Another, as yet undiscovered, constraint is required in order to define a solution (Sawford and Guest, 1988).

We attempted to find a simple solution to Equation (3) which met the conditions in (4). Equation (3) states that the divergence of probability current in the vertical is balanced by the divergence of probability current in the velocity plane. The simplest solution is to set either ϕ_u or ϕ_w to zero. Setting ϕ_u to zero gives,

$$\phi_w = -\frac{\partial}{\partial z}\int_{-\infty}^{w} wP_{uw}(z)\,\mathrm{d}w .$$

This is the unique value of ϕ_w for a one-dimensional model (Thomson, 1987; Luhar and Britter, 1989; and Weil, 1990). In this case a vertical gradient in $P_{uw}(z)$ results in a vertical acceleration of the particle via the effect of ϕ_w on a_w but would have no effect on u. Unfortunately, this leads to a violation of the conditions in (4), since a two-dimensional model ϕ_w does not in general go to zero as w becomes infinitely large (this violation would lead to infinite particle accelerations). The same problem exists if ϕ_w is set equal to zero.

The ϕ_u and ϕ_w are the u and w components of a vector $\boldsymbol{\phi}$ in the u, w phase space: $\boldsymbol{\phi} = \phi_u\mathbf{i} + \phi_w\mathbf{j}$, where $\mathbf{i}$ and $\mathbf{j}$ are unit vectors in the positive u and w directions, respectively. We considered two simple specifications of $\boldsymbol{\phi}$.

(i) $\boldsymbol{\phi}$ acts to conserve the magnitude of the velocity fluctuation vector. An arbitrary possibility would be that the $\boldsymbol{\phi}$ component of particle acceleration maintains the magnitude of the fluctuation vector, but alters its direction. With this in mind, the u, w phase space was recast in cylindrical coordinates (s, θ), where s is the magnitude and θ is the direction of the velocity fluctuation vector:

$$s = \sqrt{u^2 + w^2}, \qquad \theta = \tan^{-1}(u/w) .$$

Equation (3) now becomes:

$$\nabla \cdot \boldsymbol{\phi} = -\frac{\partial}{\partial z}(s \cos\theta P_{u,w}(z)) .$$

The $\boldsymbol{\phi}$ can be expressed in s, θ coordinates as,

$$\boldsymbol{\phi} = \phi_s \mathbf{e_s} + \phi_\theta \mathbf{e_\theta} ,$$

where $\mathbf{e_s}$ and $\mathbf{e_\theta}$ are unit vectors in the direction of increasing s and θ, respectively. In cylindrical coordinates (Spiegel, 1963),

$$\nabla \cdot \boldsymbol{\phi} = \frac{1}{s}\left[\frac{\partial}{\partial s}(s\phi_s) + \frac{\partial \phi_\theta}{\partial \theta}\right] ,$$

and the desired solution (with $\phi_s = 0$) of Equation (3) is,

$$\phi_\theta(s, \theta) - \phi_\theta(s, \theta_0) = -s^2 \frac{\partial}{\partial z}\int_{\theta_0}^{\theta} \cos\theta'\, P_{uw}(z)\, \mathrm{d}\theta' ,$$

with

$$\phi_w = -\phi_\theta \sin\theta, \qquad \phi_u = \phi_\theta \cos\theta .$$

Unfortunately this solution suffers from a lack of a boundary condition: $\phi_\theta(s, \theta_0)$ is unknown except at $s = \infty$. This solution was rejected.

(ii) $\boldsymbol{\phi}$ acts to conserve the direction of the velocity fluctuation vector. Another simple possibility would be that $\boldsymbol{\phi}$ accelerates particles either towards or away from the local mean ($u = w = 0$), while the orientation of the velocity fluctuation vector remains constant: so that $\boldsymbol{\phi}$ is oriented along a line through the origin of u, w space (Figure 1). The corresponding solution of Equation (3) (with $\phi_\theta = 0$) is,

$$\phi_s(s, \theta) = -\frac{\cos\theta}{s}\frac{\partial}{\partial z}\int_{\infty}^{s} s'^2 P_{uw}(z)\, \mathrm{d}s' , \tag{5}$$

and

$$\phi_w = \phi_s \cos\theta, \qquad \phi_u = \phi_s \sin\theta .$$

This was the specification of $\boldsymbol{\phi}$ that we used in our model. It is not completely satisfactory. Although $\phi_s \to 0$ as $s \to \infty$, there are situations where $P_{uw}(z)$ could go to zero more rapidly than ϕ_s. This would result in large accelerations at high speeds, often directed toward higher speeds. In the cases that we considered, we did not find this to be a problem. A more serious difficulty is the fact that $\phi_s \to \infty$ as $s \to 0$. We were prepared to set a low threshold value for s in the ϕ_s solution, but in practice never needed to, as particle speeds remained high and ϕ_s was well behaved.

According to Kolmogorov's theory of local isotropy, the velocity changes δu_i over a small time interval δt (δt much smaller that the Kolmogorov timescale) satisfy

$$\langle \delta u_i\, \delta u_j \rangle = \delta t C_0 \epsilon \delta_{ij} ,$$

where ϵ is the mean turbulent kinetic energy dissipation rate and C_0 is a universal

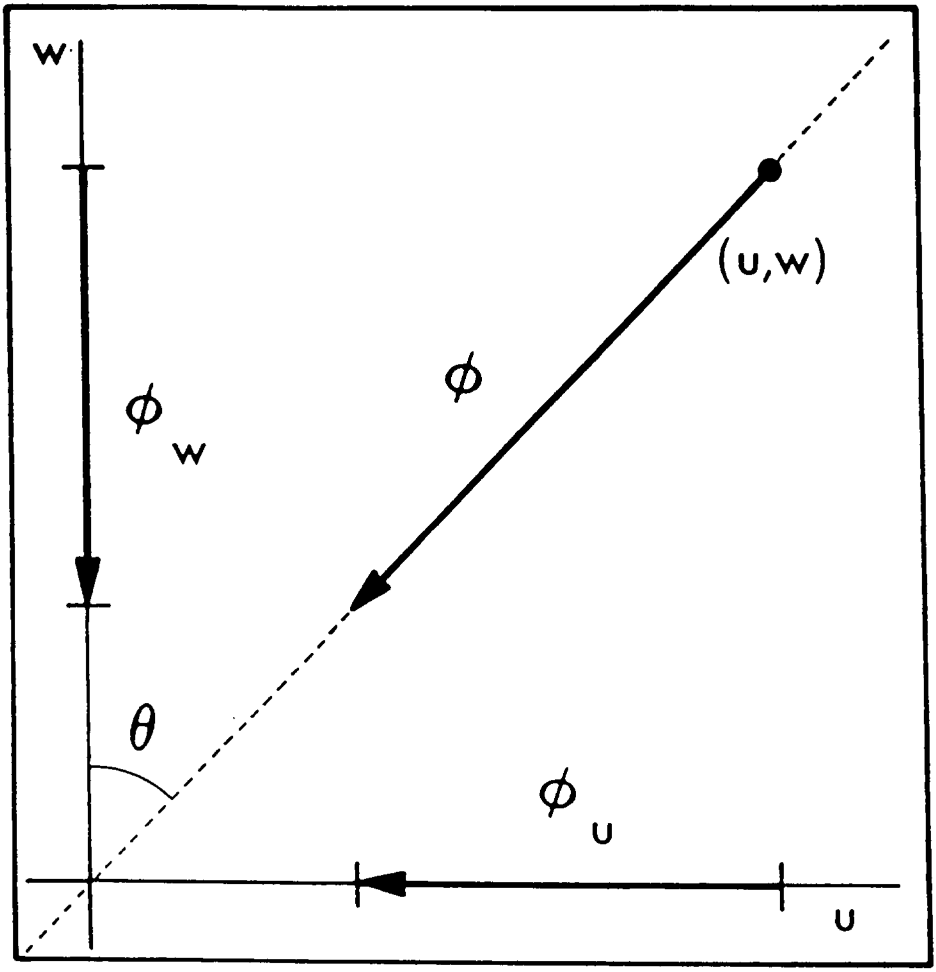

Fig. 1. Illustration of the ϕ_u and ϕ_w components of the vector ϕ in u, w phase space.

constant (experimental values of C_0 vary). For the Langevin model to obey this constraint, it is necessary that

$$b_u = b_w = \sqrt{C_0\epsilon}\,. \tag{6}$$

We have estimated $C_0\epsilon$ as $2\sigma_w^2/\tau$, where τ is the Lagrangian timescale.

2.2. Non-Gaussian PDF

We examined a bivariate Edgeworth expansion (Mardia, 1970), whose marginal distributions are of the Gram–Charlier type, as a possible method of generating the necessary non-Gaussian two-dimensional PDFs. The advantage of this method is its simplicity and flexibility in fitting any number of higher order statistical moments. Using simulated atmospheric flow statistics (Raupach *et al.*, 1986), we found that PDFs created from the Edgeworth expansion using up to third-order moments had poorly behaved tails: negative probabilities and oscillations in the PDF surface. In a trajectory-simulation model, these characteristics would likely prove disastrous. Some particles would likely move into a high velocity PDF "location" of negative probability, giving a sign reversal in a_u and a_w, and acceleration toward higher velocities. Particle behaviour will be unpredictable even in positive probability regions of the PDF tails because of the nature of the ϕ calculation in our model (integration of the PDF surface along a radial from an infinite velocity). For these reasons an Edgeworth expansion was abandoned.

In one-dimension, Baerentsen and Berkowicz (1984) constructed a non-Gaussian PDF as a linear combination of two Gaussian distributions. By varying the "weight" between the two distributions, and the distribution means and variances, they were able to correctly fit the mean, variance, and skewness of w over a range of conditions in the CBL. Following Baerentsen and Berkowicz, we constructed u, w joint-PDFs as a linear combination of two joint Gaussian distributions:

$$P_{uw}(z) = AP_A + BP_B \,, \tag{7}$$

where P_A is the Gaussian distribution:

$$P_A = \frac{1}{2\pi\sigma_{uA}\sigma_{wA}\sqrt{(1-\rho_A^2)}} \times \\ \times \exp\left[-\frac{(u-\bar{u}_A)^2\sigma_{wA}^2 + (w-\bar{w}_A)^2\sigma_{uA}^2 - 2\rho_A(u-\bar{u}_A)(w-\bar{w}_A)\sigma_{uA}\sigma_{wA}}{2\sigma_{uA}^2\sigma_{wA}^2(1-\rho_A^2)}\right], \tag{8}$$

with an analogous expression for P_B. The correlation coefficients ρ_A and ρ_B were chosen so that:

$$\rho_A = \frac{\overline{uw}}{\sigma_u\sigma_w}, \qquad \rho_B = \frac{(\overline{uw} - A\rho_A\sigma_{uA}\sigma_{wA})}{B\sigma_{uB}\sigma_{wB}}. \tag{9}$$

Equation (9) ensures the correct $\overline{uw}$ for the combined distribution. There is the potential for $|\rho_B|$ to exceed 1, although we did not encounter this problem.

Equations (7) and (8) represent a system containing 10 unknowns (A, B, $\bar{w}_A$, $\overline{W}_B$, σ_{wA}, σ_{wB}, $\bar{u}_A$, $\bar{u}_B$, σ_{uA}, σ_{uB}). We attempted to specify the unknowns by solving for the first five moments of w,

$$A\int_{-\infty}^{\infty}\int_{-\infty}^{\infty} w^n P_A \,\mathrm{d}w\,\mathrm{d}u + B\int_{-\infty}^{\infty}\int_{-\infty}^{\infty} w^n P_B \,\mathrm{d}w\,\mathrm{d}u = \overline{w^n}\,, \\ n = 0, 1, 2, 3, 4\,; \tag{10}$$

four moments of u,

$$A \int_{-\infty}^{\infty} \int_{-\infty}^{\infty} u^n P_A \, du \, dw + B \int_{-\infty}^{\infty} \int_{-\infty}^{\infty} u^n P_B \, du \, dw = \overline{u^n} , \quad n = 1, 2, 3, 4; \qquad (11)$$

and mixed moment

$$A \int_{-\infty}^{\infty} \int_{-\infty}^{\infty} uw^2 P_A \, du \, dw + B \int_{-\infty}^{\infty} \int_{-\infty}^{\infty} uw^2 P_B \, du \, dw = \overline{uw^2} . \qquad (12)$$

Using the flow statistics of the wind tunnel experiment (an artificial canopy of Raupach *et al.* (1986)) we were unable to obtain a solution for Equations (10), (11), and (12). Focusing on the mixed moment, $\overline{uw^2}$, we found that a solution required unrealistically large magnitudes of $\overline{uw^2}$. We decided to eliminate the $\overline{uw^2}$ constraint (Equation (12)), and arbitrarily define

$$\sigma_{uA}^2 = (R\bar{u}_A)^2, \qquad \sigma_{uB}^2 = (R\bar{u}_B)^2 .$$

This is similar to the assumption made by Weil (1990) for the one-dimensional case. This leaves nine unknowns $(A, B, \bar{w}_A, \bar{w}_B, \sigma_{wA}, \sigma_{wB}, \bar{u}_A, \bar{u}_B, R)$, to be solved by the nine moment equations:

$$\begin{aligned}
&A + B = 1 , \\
&A\bar{w}_A + B\bar{w}_B = 0 , \\
&A(\sigma_{wA}^2 + \bar{w}_A^2) + B(\sigma_{wB}^2 + \bar{w}_B^2) = \sigma_w^2 , \\
&A(3\sigma_{wA}^2\bar{w}_A + \bar{w}_A^3) + B(3\sigma_{wB}^2\bar{w}_B + \bar{w}_B^3) = \bar{w}^3 , \\
&A(3\sigma_{wA}^4 + 6\sigma_{wA}^2\bar{w}_A^2 + \bar{w}_A^4) + B(3\sigma_{wB}^4 + 6\sigma_{wB}^2\bar{w}_B^2 + \bar{w}_B^4) = \overline{w^4} , \qquad (13) \\
&A\bar{u}_A + B\bar{u}_B = 0 , \\
&A(\sigma_{uA}^2 + \bar{u}_A^2) + B(\sigma_{uB}^2 + \bar{u}_B^2) = \sigma_u^2 , \\
&A(3\sigma_{uA}^2\bar{u}_A + \bar{u}_A^3) + B(3\sigma_{uB}^2\bar{u}_B + \bar{u}_B^3) = \overline{u^3} , \\
&A(3\sigma_{uA}^4 + 6\sigma_{uA}^2\bar{u}_A^2 + \bar{u}_A^4) + B(3\sigma_{uB}^4 + 6\sigma_{uB}^2\bar{u}_B^2 + \bar{u}_B^4) = \overline{u^4} .
\end{aligned}$$

Equations (13) were solved by numerical methods.

Figure 2 shows a constructed PDF for a typical within-canopy case (flow statistics from Raupach *et al.*, 1986). The solution has the correct velocity means, variances, skewness, and kurtosis, and covariance. Further moments are generally not correct. The PDF illustrated in Figure 2 is clearly non-Gaussian as illustrated by the non-zero mode (located near $u = -1$ and $w = 0.3$). This PDF qualitatively agrees with observations of canopy flow: a temporal predominance of low velocity updrafts having a horizontal velocity less than the mean (quiescent periods), punctuated by high velocity downdrafts having a high horizontal velocity (sweeps).

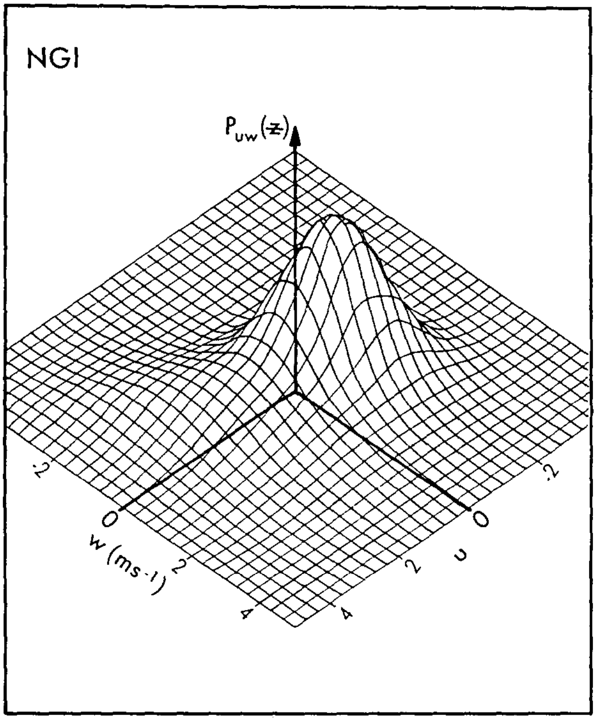

Fig. 2. Joint-probability density function for turbulent velocities (u, w) within a canopy at $z/h_c = 0.85$ formulated from the flow statistics of Raupach *et al.* (1986). The label NG1 is used to distinguish this PDF from others introduced later in the text.

2.3. Application of the Trajectory-Simulation Model

The ϕ_u and ϕ_w corresponding to our non-Gaussian PDF are given in the Appendix. In the model, vertical derivatives in ϕ_u and ϕ_w were evaluated in finite difference form. The nine PDF parameters were tabulated for 500 unevenly spaced vertical levels chosen to provide high resolution at the levels of the greatest gradients in flow statistics. For each particle trajectory step, the tabulated parameters at the nearest height were used along with uncentered "upward" height derivatives (creating a slight but quantitatively negligible bias in our derivative calculations).

The time-step (dt) was selected by comparing simulation outcomes for different values of dt. Using the flow information from Raupach *et al.* (1986), we calculated concentration profiles at several points downstream of a continuous line source using dt equal to 0.1τ, 0.05τ, 0.025τ, 0.01τ, and 0.005τ. The profiles showed little systematic change for time-steps below 0.05τ. For our simulations we selected $dt = 0.025\tau$.

The ground was taken to be a perfect reflector. When the particle reached the ground (actually a roughness height just above the ground) it was "bounced", and the sign of w was reversed. This simple reflection scheme is questionable in non-Gaussian turbulence. Asymmetry of the PDF makes it possible that a sign reversal of w would result in an "invalid" w (or joint u, w velocity). Weil (1990) addressed this problem in a one-dimensional model by choosing a reflected positive velocity ($w+$) that preserves the "cumulative negative probability" of the negative "impact" velocity ($w-$):

$$\frac{\int_{w+}^{0} P_w \, \mathrm{d}w}{\int_{\infty}^{0} P_w \, \mathrm{d}w} = \frac{\int_{0}^{w-} P_w \, \mathrm{d}w}{\int_{0}^{-\infty} P_w \, \mathrm{d}w} .$$

Experimenting with different reflection schemes revealed a general insensitivity of our model results to reflection. This was due to the fact that reflection was not a frequent occurrence when within-canopy profiles were imposed. Incorporating flow statistics near the ground (decreasing velocity variances with decreasing height) creates a barrier to model particles, even without resolving a sublayer at the ground across which variance vanishes. Perhaps using more realistic flow statistics and an appropriately reduced timestep near the ground may eliminate the need for a reflection scheme (ground unattainable).

3. Model Comparisons with Experiments

3.1. Tavoularis and Corrsin Line Source Experiment

Tavoularis and Corrsin (1981), hereafter referred to as TC, studied dispersion of heat from a line source in linearly sheared wind tunnel flow. A heated wire was placed perpendicular to the mean flow at a height $z_{src} = 0.55h_t$ (h_t is the height of the wind tunnel). The turbulence was slightly non-Gaussian ($\mathrm{Sk}_w = 0.16$, $\mathrm{Sk}_u = -0.22$, $\mathrm{Kt}_w = 3.2$, $\mathrm{Kt}_u = 3.1$). Although not representative of canopy flow, its approximate homogeneity makes it a good test for the effects of skewness and kurtosis on dispersion because the ϕ_u and ϕ_w terms in our trajectory-simulation model vanish.

We compared the TC temperature profiles with our model predictions at a fetch $x = 5.0h_t$. Unfortunately the heat source strength and the Lagrangian timescale were not specified, limiting the information which can be extracted. We ran the model with $\tau = 0.042s$, approximated from a formula suggested by TC:

$$\tau \approx 5\frac{\lambda}{\sigma_u}, \qquad \lambda = \sqrt{\frac{\sigma_u^2}{(\partial u/\partial x)^2}} .$$

We then normalized the predicted temperature profiles with the peak temperature.

The addition of skewness and kurtosis to the PDF improves the prediction of

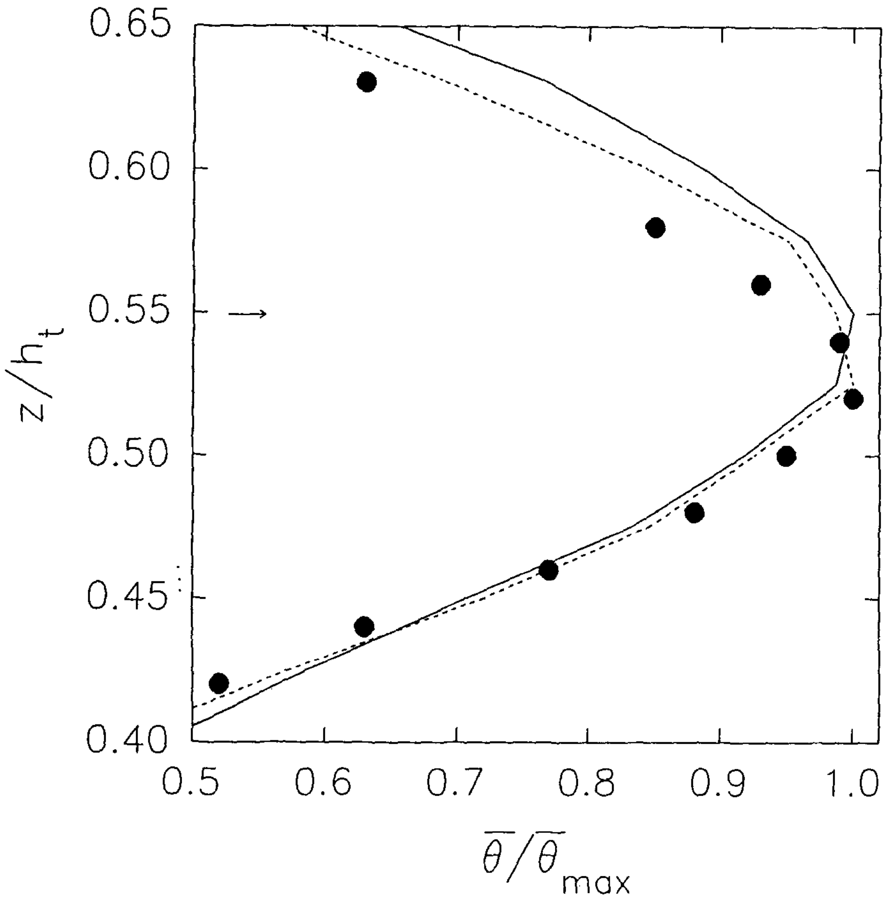

Fig. 3. Comparison of normalized temperature measurements from the TC experiment (·) with predicted values using Gaussian (———) and non-Gaussian (-------) PDFs. Source height is indicated by the →.

the peak temperature location (Figure 3), which is the only aspect of the TC profile whose simulation is not sensitive to the specification of τ and source strength. The Gaussian model maintains the temperature peak at z_{src}, while skewness and kurtosis act to lower peak location. The difference in peak location was statistically significant ($P = 0.05$, paired t-test), although the concentration profiles were not statistically different near the temperature peak. These results were anticipated, because a positive Sk_w indicates a temporal predominance of low velocity downdrafts, balanced by high velocity updrafts. This would move the majority of particles initially downward from the source, as compared to a Gaussian balance between upward and downward, and reduce the height of the peak temperature (the shear in mean horizontal velocity also acts to lower the temperature peak). It should be noted that in the TC flow, Sk_w is positive and Sk_u is negative, while within a canopy the signs are reversed. Therefore within a canopy skewness would be expected to move the peak concentration upward (while mean horizontal velocity shear moves it downward).

Judging by the results of model predictions of the TC data, it appears that in even slightly non-Gaussian flow, a consideration of non-Gaussian characteristics may be important in predicting certain dispersion features.

3. The Legg, Raupach, and Coppin Line Source Experiment

The experiment of Legg, Raupach, and Coppin (1986), hereafter referred to as LRC, examined dispersion within and above an artificial crop in a boundary-layer wind tunnel. Heat was released as a tracer from an elevated line source located perpendicular to the flow within the canopy at a source height $z_{src} = 0.85h_c$ (h_c is the canopy height). Flow within and above the canopy was inhomogeneous and non-Gaussian (Raupach *et al.*, 1986): this was representative of a real canopy and a good test for our model.

The flow statistics we used in our model simulation of LRC were drawn from Raupach *et al.* (1986) and are shown in Figure 4. The 500 vertical levels of the model parameter table were chosen such that 400 were evenly spaced from a reflecting boundary at $z = 0.067h_c$ to $z = 2.067h_c$. The remaining 100 levels were evenly spaced up to $z = 3.72h_c$. Above this height the flow was taken to be homogeneous.

An important comparison which can be made for the inhomogeneous LRC flow is between the results of Thomson's (1987) Gaussian model and our model using Gaussian PDFs. Thomson's a_u and a_w are:

$$a_u = -\frac{1}{2(\sigma_u^2\sigma_w^2 - \overline{uw}^2)}\, b_u^2[\sigma_w^2 u - \overline{uw}w] + \frac{\phi_u}{P_{uw}(z)},$$

$$a_w = -\frac{1}{2(\sigma_u^2\sigma_w^2 - \overline{uw}^2)}\, b_w^2[-\overline{uw}u + \sigma_u^2 w] + \frac{\phi_w}{P_{uw}(z)},$$

with

$$\frac{\phi_u}{P_{uw}(z)} = \frac{1}{2}\frac{\partial(\overline{uw})}{\partial z} + w\frac{\partial U}{\partial z} + \frac{1}{2(\sigma_u^2\sigma_w^2 - \overline{uw}^2)} \times$$
$$\times \left[\sigma_w^2 \frac{\partial \sigma_u^2}{\partial z} uw - \overline{uw}\frac{\partial \sigma_u^2}{\partial z} w^2 - \overline{uw}\frac{\partial(\overline{uw})}{\partial z} uw + \sigma_u^2 \frac{\partial(\overline{uw})}{\partial z} w^2\right],$$

$$\frac{\phi_w}{P_{uw}(z)} = \frac{1}{2}\frac{\partial \sigma_w^2}{\partial z} + \frac{1}{2(\sigma_u^2\sigma_w^2 - \overline{uw}^2)} \times$$
$$\times \left[\sigma_w^2 \frac{\partial(\overline{uw})}{\partial z} uw - \overline{uw}\frac{\partial(\overline{uw})}{\partial z} w^2 - \overline{uw}\frac{\partial \sigma_w^2}{\partial z} uw + \sigma_u^2 \frac{\partial \sigma_w^2}{\partial z} w^2\right].$$

Notice the vertical derivative of the mean horizontal velocity (U) in ϕ_u: Thomson's

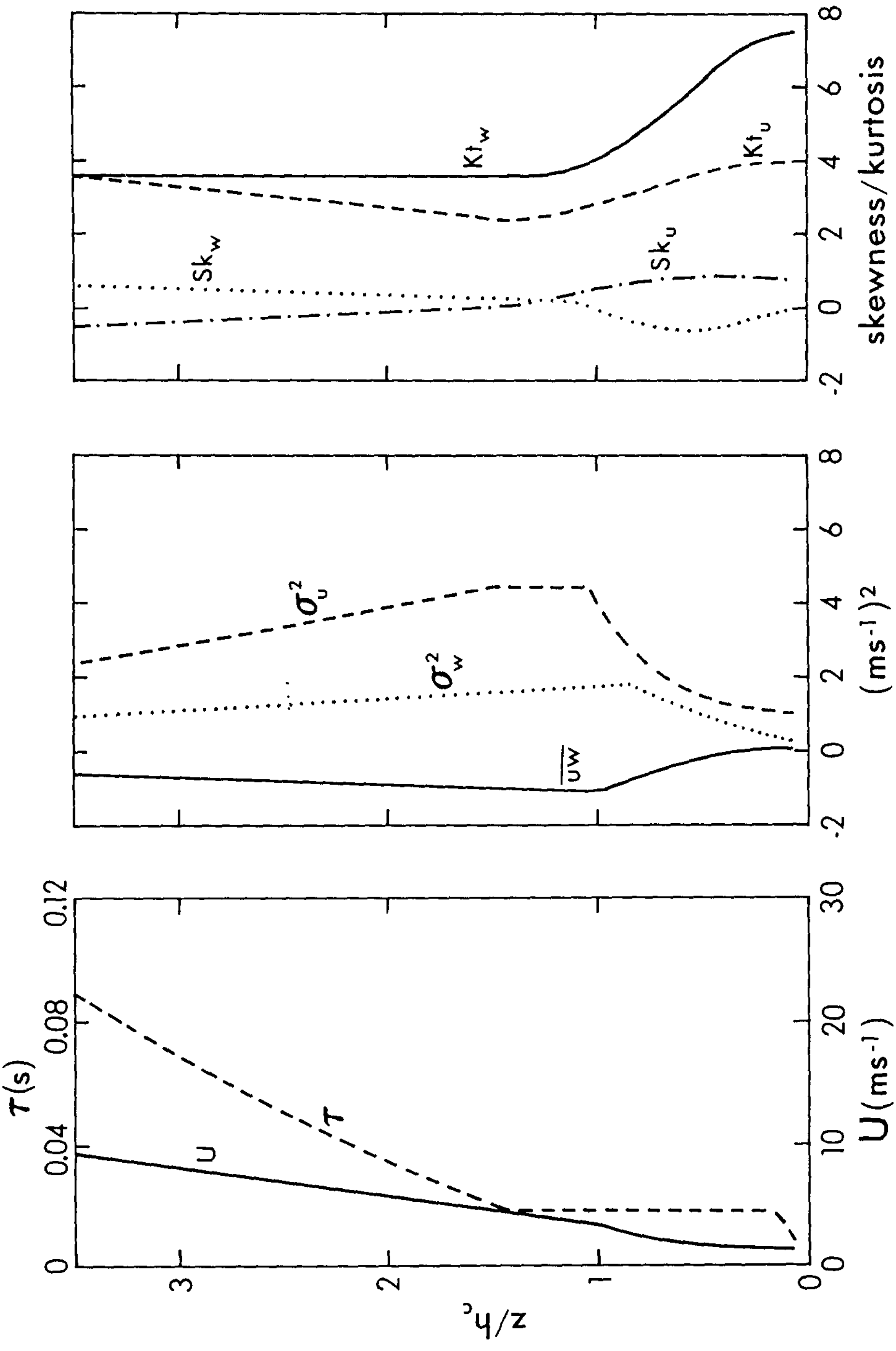

Fig. 4. Flow statistics used in the trajectory-simulation model for the LRC and CRL experiments.

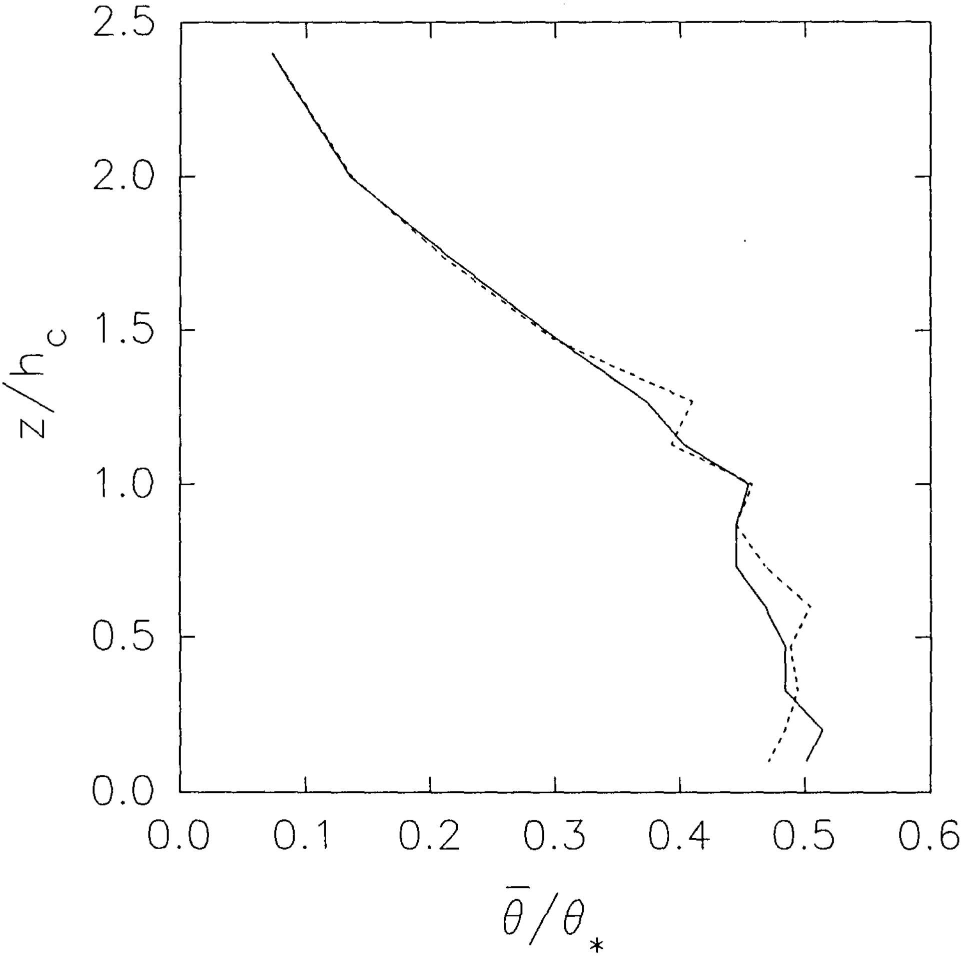

Fig. 5. Comparison of predicted temperature profiles for our model using Gaussian PDFs (———) with Thomson's (1987) Gaussian model (-------) at a fetch $x = 2.78h_c$.

Langevin equation determines the change in total velocity $(U + u)$, not just the change in the fluctuating component as does ours. The ϕ_u and ϕ_w terms in Thomson's model differ significantly from ours. This difference must occur to allow for a non-Gaussian PDF. Although it may be possible that some formulation of ϕ relaxes to Thomson's model in the Gaussian case, ours does not. We ran Thomson's model with the b_u and b_w values given by Equation (6). Concentration profiles computed using our model were not statistically different (paired t-test, $P = 0.05$) from those predicted by Thomson's model at fetches $x = 0.38h_c$, $2.78h_c$, and $11.60h_c$ (Figure 5). That these two different models, both satisfying the well-mixed criteria, gave statistically the same results may indicate a general insensitivity to the exact form of ϕ in a model developed from the well-mixed criteria.

Comparisons of the LRC temperature profiles with our model predictions using both Gaussian and non-Gaussian PDFs were made at fetches of $x = 0.38h_c$, $2.78h_c$, and $11.60h_c$ (Figure 6). There was good agreement between the LRC measurements and the Gaussian model. Given the standard error of the model predictions and the observed scatter in the LRC data, only in the regions just above the canopy at $x = 2.78h_c$, and just above the ground at $x = 0.38h_c$, could the model predictions be considered significantly different from the LRC measurements. This is surprising, given the complex, non-Gaussian flow within and above the canopy. The model underprediction just above the ground may be the result of experimental complications. The plume centroid at the source ($x = 0$) was measured by LRC to lie significantly below z_{src} and they suggest that a possible explanation is the existence of an organized recirculating flow (caused by canopy elements) which resulted in upstream heat transport in the lower canopy. If this is the case, temperature underprediction near the ground would be unavoidable.

The performance of the non-Gaussian model was poor. At all three fetches the non-Gaussian model temperature predictions were not as good as the Gaussian. At $x = 0.38h_c$ and $2.78h_c$ the non-Gaussian model underpredicted temperature below z_{src} and overpredicted temperature immediately above z_{src}. The difference between the Gaussian and non-Gaussian predictions at these fetches was statistically significant ($P = 0.05$) at most heights. At $x = 11.6h_c$ the differences between the Gaussian and non-Gaussian models are smaller, and below $z = 2h_c$ the model results were not statistically different. But at greater heights the results of the two models remain different.

The non-Gaussian model predictions were disappointing because the change from Gaussian to non-Gaussian profiles seems consistent with the present view of canopy flow. The flow in LRC is characterized by negative Sk_w. In this flow, low velocity updrafts would be temporally dominant. This is a well-known characteristic of canopy flow: a predominance of low velocity updrafts, punctuated by occasional high velocity downdrafts (increasing kurtosis reduces the "peakiness" of the distribution). Therefore a negative Sk_w should shift the final particle distribution upwards, with a larger peak just above the source when compared with the Gaussian case. This was just what was seen in the modelled temperature profile (the reverse was observed in the positively skewed TC flow).

In addition to the temperature profiles, we compared model predictions of the horizontal turbulent heat flux ($\overline{u\theta}$) with the LRC measurements at $x = 0.38h_c$ and $2.78h_c$ (Figure 7). The results confirm the superiority of the Gaussian model over the non-Gaussian model. At most heights the Gaussian predictions were not statistically different from measurement values, while the non-Gaussian predictions were statistically different near z_{src} at $x = 0.38h_c$ and just above the canopy at $x = 2.78h_c$. At larger fetches $\overline{u\theta}$ predictions for both models approach zero, agreeing with experimental results.

3.3. The Coppin, Raupach, and Legg Planar Source Experiment

The experiment of Coppin, Raupach, and Legg (1986), hereby referred to as CRL, was part of the same series as LRC. Using the same wind tunnel arrangement, CRL

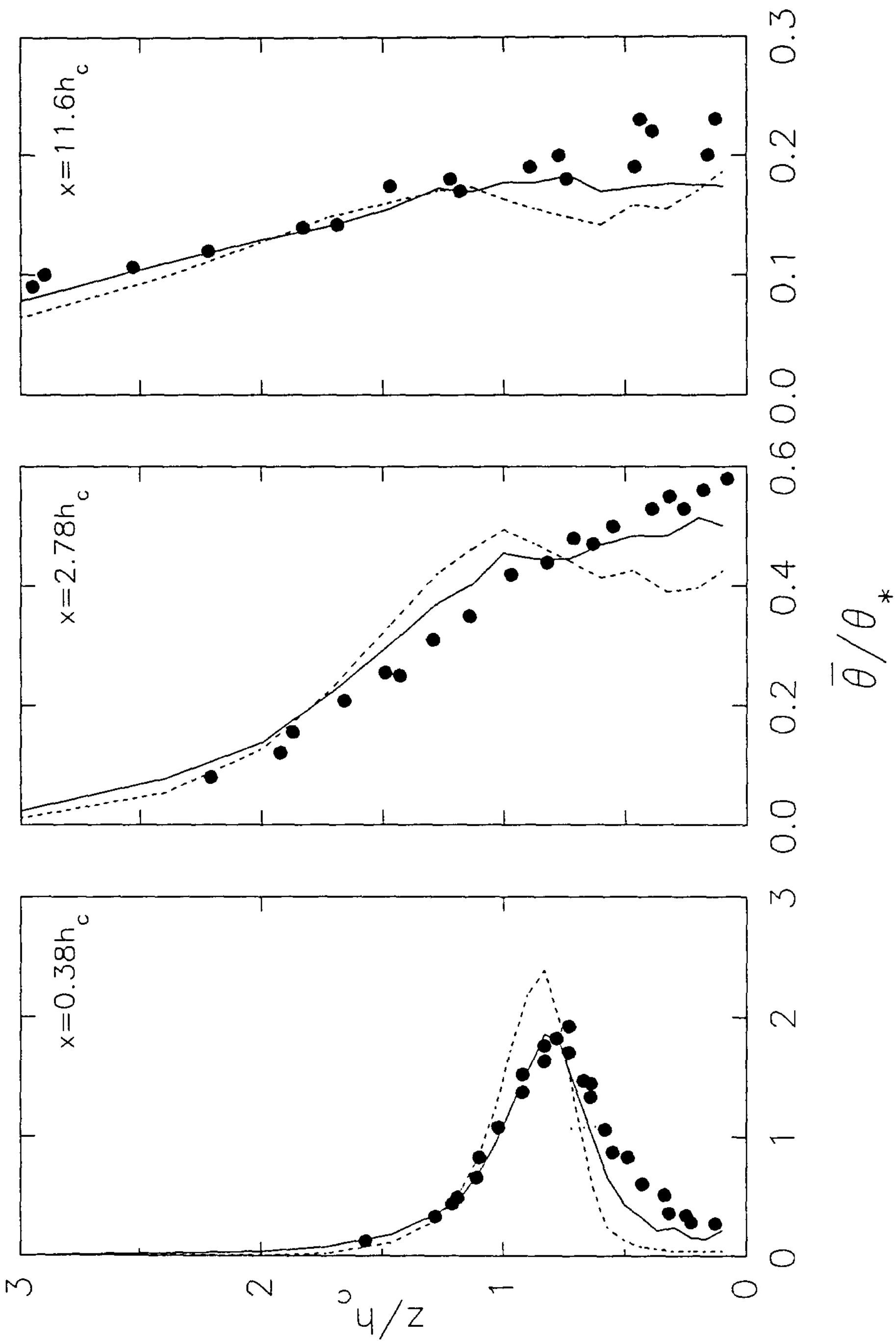

Fig. 6. Comparison of normalized temperature measurements from the LRC experiment (·) with predicted values using Gaussian (——) and non-Gaussian (------) PDFs at three fetches (*x*).

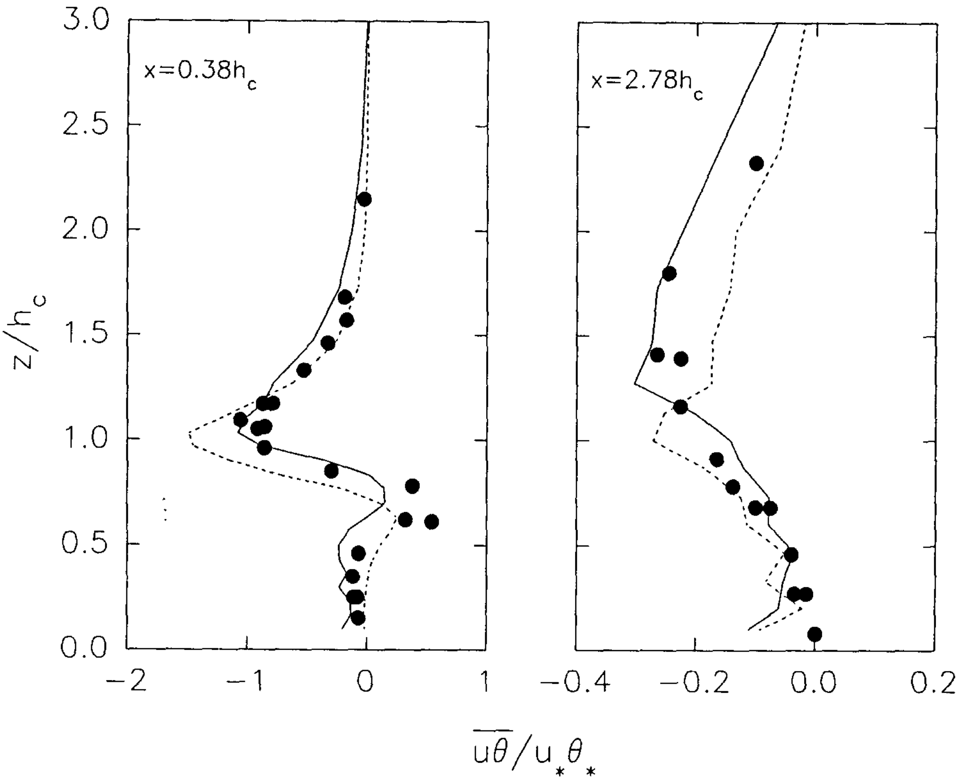

Fig. 7. Comparison of normalized horizontal turbulent heat flux measurements from the LRC experiment (·) with predicted values using Gaussian (———) and non-Gaussian (-------) PDFs at two fetches (x).

constructed a planar heat source from an array of heated wires at height $z_{src} = 0.80h_c$. The trajectory-simulation details for CRL were identical to the simulation of the LRC experiment. Model temperature profiles were compared with measured values at fetches of $x = 8.8h_c$ and $33.8h_c$ (Figure 8).

Since a planar source is a superposition of line sources with differing fetches, model temperature profiles were essentially a hybridization of the three line source profiles of LRC that we have shown. At $x = 8.8h_c$ the temperature was underpredicted below z_{src} by both the Gaussian and non-Gaussian model, consistent with model predictions of LRC at the shortest fetch. The overprediction in the peak temperature and peak height by the non-Gaussian model when compared with the Gaussian model agree with the LRC simulations. Predicted temperature profiles improve for both models at the longer fetch ($x = 33.8h_c$), with the Gaussian model giving good predictions. This improvement was due to a proportional reduction in the heat contribution from the source area nearest the measurement location. As seen with the LRC simulations, the model predictions are better farther from the source.

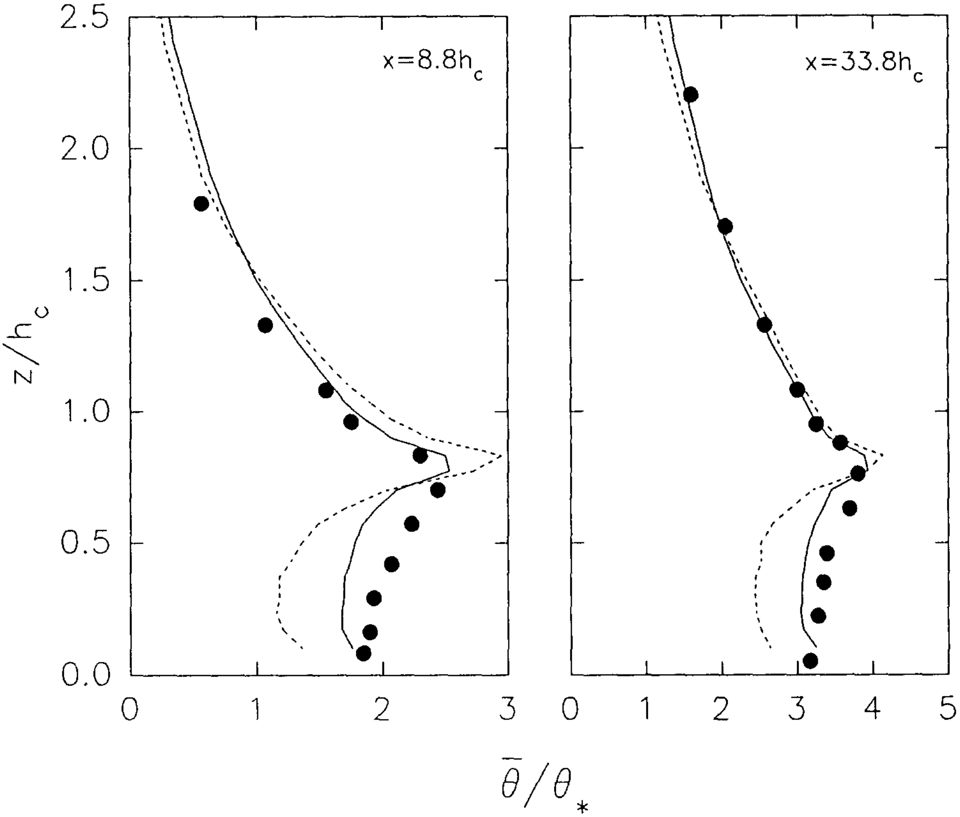

Fig. 8. Comparison of normalized temperature measurements from the CRL experiment (·) with predicted values using Gaussian (———) and non-Gaussian (-------) PDFs at two fetches (x).

3.4. The sensitivity of model results to PDF formulation

The inferiority of the non-Gaussian model (relative to the Gaussian) in predicting dispersion in inhomogeneous turbulence (LRC and CRL) was surprising. Assuming that the experimental measurements were correct, poor performance of the non-Gaussian model could have occurred because the underlying Lagrangian stochastic model was incorrect, or because the PDFs formulated for use with the model were incorrect. At present there are no criteria for judging the validity of any particular Lagrangian model which satisfies the well-mixed criterion other than by the extent of agreement with experiment, and the effects of the model assumptions and the PDF assumptions are not easily separable. A possible clue to the cause of poor simulations is the sensitivity to PDF characteristics.

Three different non-Gaussian PDF profiles (NG1, NG2, and NG3), having similiar moments, were "constructed" for the simulation of the LRC experiment. Profile NG1 was the standard profile used for our previous simulations. Profiles NG2 and NG3 result from redefining σ_{uB},

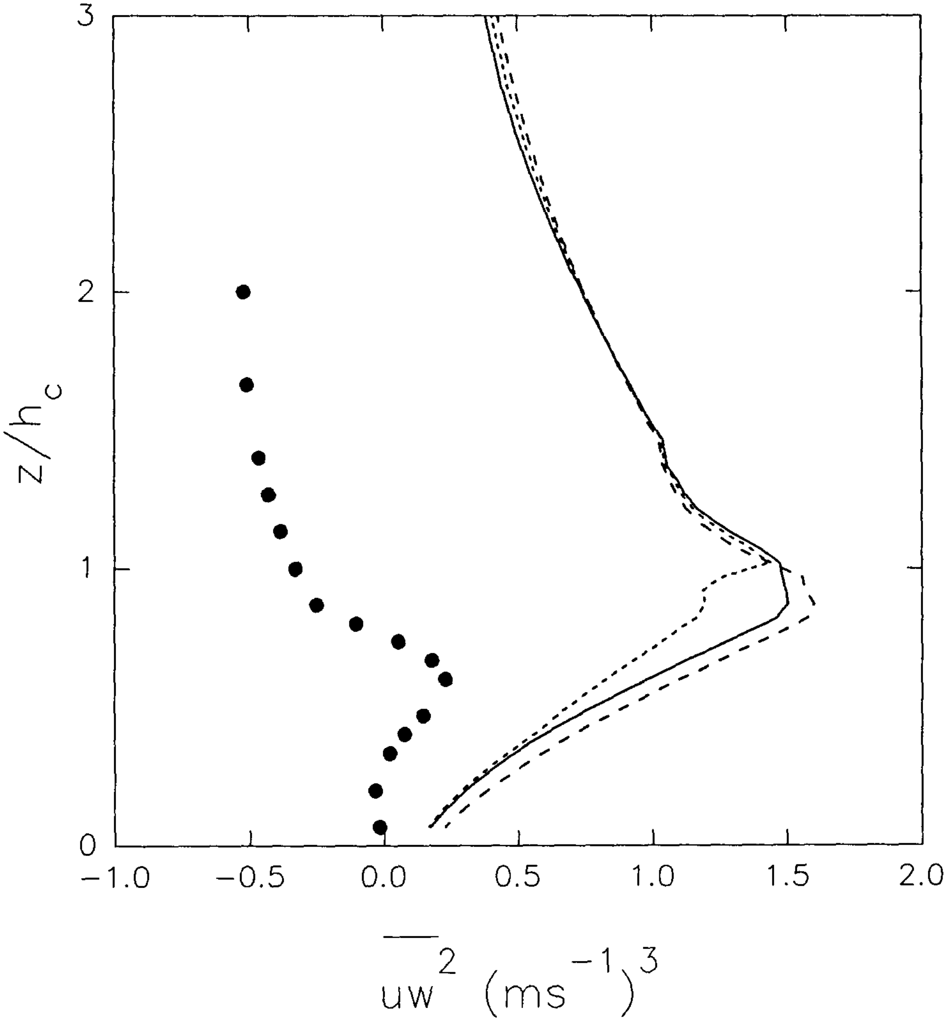

Fig. 9. Comparison of measured $\overline{uw^2}$ (·) from the LRC experiment with values from the non-Gaussian PDF profiles NG1 (———), NG2 (-------), and NG3 (············).

$$\sigma_{uB} = \alpha R \overline{u_B} \, ,$$

and solving Equations (13). Profile NG2 corresponds to $\alpha = 0.8$, and NG3 to α variable with height ($\alpha = 0.8$ to 1.8). Each of the three PDF profiles had the correct u and w mean, variance, skewness, and kurtosis, and the correct $\overline{uw}$; but other higher order moments differ. Figure 9 shows the difference in $\overline{uw^2}$ for the three profiles and their large difference from the measured values. Figure 10 shows the dramatic difference in PDFs between NG2 and NG3 at a height $z/h_c = 0.85$, which can be compared with the similiar PDF for NG1 in Figure 2. Clearly, higher order moments are important in defining a PDF.

Model simulations of the LRC experiment using the three non-Gaussian PDFs

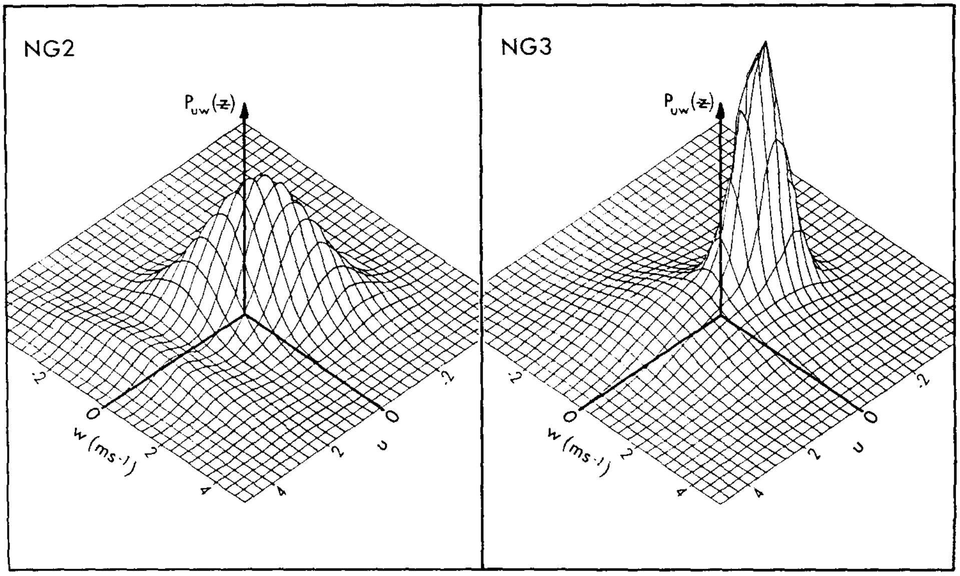

Fig. 10. Non-Gaussian velocity (u, w) PDFs, from the PDF profiles NG2 and NG3, corresponding to height $z/h_c = 0.85$ in the LRC experiment.

yielded large differences in concentration profiles at fetch $x = 0.38h_c$ (Figure 11). The modelled concentration profile from NG3 was significantly different from NG1 and NG2, with a peak concentration above the source height. This is due to the much narrower velocity region of high probability in NG3 at the source height, centered at $u = -1.30$, $w = 0.35$ (Figure 10). Therefore most particles moved slowly upward from the source. The NG3 PDF also had a greater probability of large negative w than NG1 and NG2, giving higher ground-level concentrations.

Higher order PDF moments can certainly affect the simulated dispersion of a trajectory-simulation model. The differences in concentration profile resulting from PDF differences show that attempts to increase the accuracy of dispersion models by creating more accurate PDFs will require formulations having accuracy over a range of higher order moments. The differences also suggest that the poor performance of the non-Gaussian model in the LRC and CRL experiment is at least partially due to errors in our PDF formulations.

4. Summary and Conclusions

A two-dimensional trajectory-simulation model (which was consistent with Thomson's (1987) well-mixed criterion) was developed. We assumed a simple form for the "probability current" (ϕ) which satisfies the probability continuity equation in the u, w, z phase space, namely that $\phi/P_{uw}(z)$ accelerates particles directly towards (or away from) the origin of (u, w) space. For Gaussian turbulence the

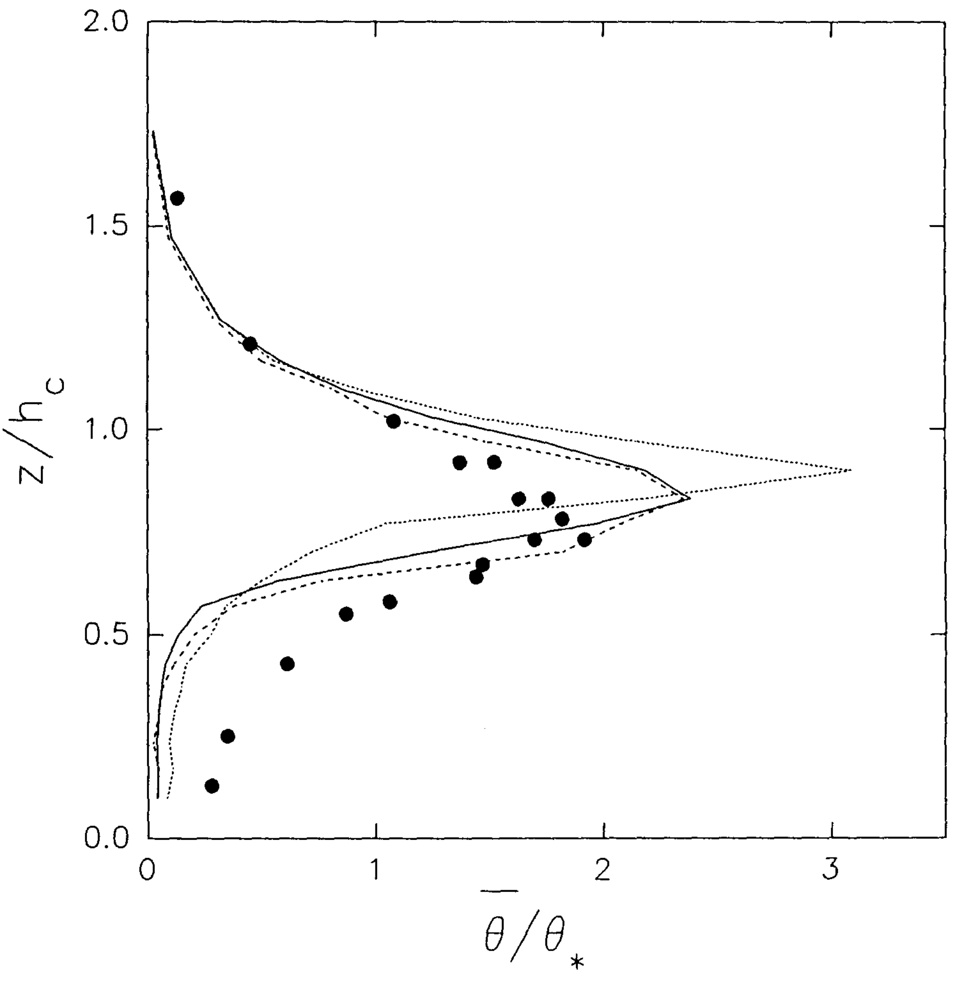

Fig. 11. Comparison of the LRC temperature measurements (·) with predicted values using the non-Gaussian PDF profile NG1 (———), NG2 (-------) and NG3 (············) at a fetch $x = 0.38h_c$.

model gave results which were in statistical agreement with the multi-dimensional Gaussian model of Thomson (1987).

The novelty of our trajectory-simulation model is that it permits non-Gaussian velocity statistics, a characteristic of flow within and above plant canopies. The effect of non-Gaussian turbulence on dispersion was examined by creating non-Gaussian u, w probability density functions (PDFs) by summing two Gaussian PDFs. The individual Gaussian parameters were selected so that the resultant PDF had the correct u and w mean, variance, skewness, and kurtosis, and the correct covariance. Other moments were generally not correct.

Comparisons of the model results with wind-tunnel dispersion experiments showed that in homogeneous, slightly non-Gaussian turbulence (TC experiment), the incorporation of skewness and kurtosis in the PDF resulted in correct prediction of the height of the concentration peak downwind of a line source. But in the much more complex case of inhomogeneous, highly non-Gaussian turbulence (LRC and CRL experiments) typical of flow within a plant canopy, the addition of skewness and kurtosis in the model resulted in substantially worse agreement with experimental data.

Although the poor results of the non-Gaussian model may be the result of an incorrect Lagrangian stochastic model, we believe that poorly formulated PDFs are the more likely cause. The agreement between the results of our model with Gaussian statistics and Thomson's (1987) Gaussian model, which have very different ϕ, suggest to us an insensitivity to the exact form of a model developed from the well-mixed condition. But our results clearly show the sensitivity of our model to PDF differences. At first it seems improbable that extending the accuracy of a PDF to the individual third and fourth moments (skewness and kurtosis) would reduce the accuracy achieved by the Lagrangian stochastic model, but the generality of a PDF constructed from two Gaussian PDFs is limited. Correctly fitting some of the moments constrains other moments to values which may not be realistic. For instance, in the case of the LRC and CRL experiments (highly non-Gaussian turbulence), the absolute errors in $\overline{uw^2}$ (which were not used to fit the PDFs) were much greater for our non-Gaussian PDFs than for the Gaussian PDFs (where $\overline{uw^2} = 0$). Unfortunately, even small errors in individual u, w PDFs may lead to substantial errors in estimating PDF spatial derivatives (which define ϕ_u and ϕ_w). For homogeneous flow the impact of incorrect PDFs is limited, as the PDF spatial derivatives vanish ($\phi_u = \phi_w = 0$), and particle acceleration is determined by the u and w derivatives of the PDF; in any realistic PDF formulation these derivatives should be well behaved, resulting in acceleration towards the local mean. But for inhomogeneous flows ϕ_u and ϕ_w can dominate the calculation of particle acceleration, and PDF errors can have a dramatic effect. Our results suggest that for inhomogeneous flow, attempts to increase the accuracy of trajectory-simulation models by using more accurate PDFs will require the development of very accurate PDF formulations.

But the development of improved PDF formulations may prove to be a wasted effort. The surprising accuracy of the Gaussian model in the complex non-Gaussian flow seems to indicate that the effects of skewness and kurtosis on mean absolute dispersion within a canopy are minor. Although others have shown that skewness affects dispersion importantly in the CBL (a simpler flow than found within canopies), and we found that the addition of skewness and kurtosis improved prediction in homogeneous turbulence, in highly inhomogeneous flow skewness and kurtosis may have a minimal effect when compared with other factors such as the strong vertical gradients in velocity variance and shear stress. In fact it may be unrealistic to add greater detail to PDFs when underlying model assumptions such as stationarity and horizontal homogeneity are not satisfied by the flow (environmental flows are rarely truly stationary; and even wind tunnel flows present to a drifting particle, horizontal inhomogeneity in mean properties).

In conclusion it appears that a two-dimensional Gaussian model, such as ours or Thomson's (1987), is very accurate in modelling dispersion in the inhomogeneous, non-Gaussian turbulence within and above a plant canopy. Our efforts to include non-Gaussian statistics resulted in a much more complex model (requiring much greater computation time), and gave less accurate results. We believe that this is due to limitations in our formulation of non-Gaussian PDFs. Until additional dispersion experiments in complex flow show otherwise, we believe a multi-dimensional Gaussian Lagrangian approach represents the most accurate method of modelling within canopy dispersion.

Acknowledgements

The authors are grateful to Geoff Lester for preparing the manuscript figures. The useful comments of an anonymous reviewer were also appreciated.

Appendix

The ϕ_u and ϕ_w terms in our non-Gaussian trajectory simulation model are found by elementary but tedious algebra. The solution for ϕ_u and ϕ_w as given in the text is:

$$\phi_u = \phi_s \sin\theta, \qquad \phi_w = \phi_s \cos\theta,$$

where (Equation (5)),

$$\phi_s = -\frac{\cos\theta}{s}\frac{\partial}{\partial z}\int_{\infty}^{s} s'^2 P_{uw}(z)\,\mathrm{d}s' . \tag{A-1}$$

with

$$s = \sqrt{u^2 + w^2}, \qquad \theta = \tan^{-1}(u/w) .$$

Inserting our non-Gaussian PDF (Equations (7) and (8) expressed in s, θ coordinates) into (A-1) yields the following solution:

$$\phi_s = \frac{\partial}{\partial z}\left\{\frac{A\cos\theta}{K_A s}\exp\left(\frac{M_A^2 - L_A N_A}{L_A}\right)\left\{\sqrt{\frac{\pi}{L_A}}\left[\frac{M_A^2}{2L_A^2} + \frac{1}{4L_A}\right]\times\right.\right.$$

$$\times\left[1 - \mathrm{erf}\left(\sqrt{L_A}s + \frac{M_A}{\sqrt{L_A}}\right)\right] - \left[\frac{M_A}{2L_A^2} - \frac{s}{2L_A}\right]\times$$

$$\left.\times\exp\left[-\left(\sqrt{L_A}s + \frac{M_A}{\sqrt{L_A}}\right)^2\right]\right\} + \frac{B\cos\theta}{K_B s}\exp\left(\frac{M_B^2 - L_B N_B}{L_B}\right)\times$$

$$\times \left\{ \sqrt{\frac{\pi}{L_B}} \left[\frac{M_B^2}{2L_B^2} + \frac{1}{4L_B} \right] \left[1 - \mathrm{erf}\left(\sqrt{L_B} s + \frac{M_B}{\sqrt{L_B}} \right) \right] - \left[\frac{M_B}{2L_B^2} - \frac{s}{2L_B} \right] \exp\left[- \left(\sqrt{L_B} s + \frac{M_B}{\sqrt{L_B}} \right)^2 \right] \right\} , \quad \text{(A-2)}$$

with

$$K_A = 2\pi\sigma_{uA}\sigma_{wA}\sqrt{1 - \rho_A^2} ,$$

$$L_A = \frac{(\sigma_{wA}^2 \sin^2\theta + \sigma_{uA}^2 \cos^2\theta - 2\rho_A\sigma_{uA}\sigma_{wA}\sin\theta\cos\theta)}{2\sigma_{uA}^2\sigma_{wA}^2(1 - \rho_A^2)} ,$$

$$M_A = \frac{(\rho_A\sigma_{uA}\sigma_{wA}\bar{w}_A \sin\theta - \bar{u}_A\sigma_{wA}^2 \sin\theta + \rho_A\sigma_{uA}\sigma_{wA}\bar{u}_A\cos\theta - \bar{w}_A\sigma_{uA}^2\cos\theta)}{2\sigma_{uA}^2\sigma_{wA}^2(1 - \rho_A^2)} ,$$

$$N_A = \frac{(\bar{u}_A^2\sigma_{wA}^2 + \bar{w}_A^2\sigma_{uA}^2 - 2\rho_A\sigma_{uA}\sigma_{wA}\bar{u}_A\bar{w}_A)}{2\sigma_{uA}^2\sigma_{wA}^2(1 - \rho_A^2)} .$$

The "B" subscript on the terms in Equation (A-2) indicates the use of the "B" parameters instead of the "A" parameters shown in the above terms.

References

Amiro, B. D.: 1990, 'Comparison of Turbulence Statistics within Three Boreal Forest Canopies', *Boundary-Layer Meteororol.* **51**, 99–121.

Baerentsen, J. H. and Berkowicz, R.: 1984, 'Monte Carlo Simulation of Plume Dispersion in the Convective Boundary Layer', *Atmos. Environ.* **18**, 701–712.

Baldocchi, D. D. and Meyers, T. P.: 1989, 'The Effects of Extreme Turbulent Events on the Estimation of Aerodynamic Variables in a Deciduous Forest Canopy', *Agric. Forest Meteorol.* **48**, 117–134.

Coppin, P. A., Raupach, M. R. and Legg, B. J.: 1986, 'Experiments on Scalar Dispersion Within a Model Plant Canopy, Part II: An Elevated Plane Source', *Boundary-Layer Meteorol.* **35**, 167–191.

de Baas, A. F., van Dop, H. and Nieuwstadt, F. T. M.: 1986, 'An Application of the Langevin Equation for Inhomogeneous Conditions to Dispersion in a Convective Boundary Layer', *Quart. J. R. Meteorol. Soc.* **112**, 165–180.

Durbin, P. A.: 1983, 'Stochastic Differential Equations and Turbulent Dispersion', *NASA reference publication* 1103.

Durbin, P. A.: 1984, 'Comments on Papers by Wilson *et al.* (1981) and Legg and Raupach (1982)', *Boundary-Layer Meteorol.* **29**, 409–411.

Gardiner, C. W.: 1983, *Handbook of Stochastic Processes for Physics, Chemistry and the Natural Sciences*, Springer-Verlag, Berlin, 442 pp.

Hall, C. D.: 1975, 'The Simulation of Particle Motion in the Atmosphere by a Numerical Random Walk Model', *Quart. J. R. Meteorol. Soc.* **101**, 235–244.

Hanna, S. R.: 1978, 'A Statistical Diffusion Model for use with Variable Wind Fields', *Proceedings of the AMS Fourth Symposium on Turbulent Diffusion and Air Pollution*, Boston, pp. 14–18.

Janicke, L.: 1983, 'Particle Simulation of Inhomogeneous Turbulent Diffusion', *Air Pollution Modelling and its Applications II*, Plenum, New York, pp 527–535.

Leclerc, M. Y., Thurtell, G. W. and Kidd, G. E.: 1988, 'Measurements and Langevin Simulations of Mean Tracer Concentration Fields Downwind from a Circular Line Source Inside an Alfalfa Canopy'. *Boundary-Layer Meteorol.* **43**, 287–308.

Leclerc, M. Y., Beissner, K. C., Shaw, R. H., den Hartog, G. and Neumann, H. H.: 1991, 'The Influence of Buoyancy on Third-order Turbulent Velocity Statistics within a Deciduous Forest', *Boundary-Layer Meteorol.* **55**, 109–123.

Legg, B. J.: 1983, 'Turbulent Dispersion from an Elevated Line Source: Markov Chain Simulations of Concentration and Flux Profiles', *Quart. J. R. Meteorol. Soc.* **109**, 645–660.

Legg, B. J. and Raupach, M. R.: 1982, 'Markov-chain Simulation of Particle Dispersion in Inhomogeneous Flows: the Mean Drift Velocity Induced by a Gradient in the Eulerian Velocity Variance', *Boundary-Layer Meteorol.* **24**, 3–13.

Legg, B. J., Raupach, M. R. and Coppin, P.: 1986, 'Experiments on Scalar Dispersion within a Model Plant Canopy, Part III: an Elevated Line Source', *Boundary-Layer Meteorol.* **35**, 277–302.

Luhar, K. and Britter, R. E.: 1989, 'A Random Walk Model for Dispersion in Inhomogeneous Turbulence in a Convective Boundary Layer', *Atmos. Environ.* **23**, 1911–1924.

Mardia K. V.: 1970, *Families of Bivariate Distributions*, Charles Griffin and Company Limited, London, 109 pp.

Raupach, M. R.: 1989, 'A Practical Lagrangian Method for Relating Scalar Concentrations to Source Distributions in Vegetative Canopies', *Quart. J. R. Meteorol. Soc.* **115**, 609–632.

Raupach, M. R., Coppin, P. A. and Legg, B. J.: 1986, 'Experiments on Scalar Dispersion within a Model Plant Canopy, Part I: The Turbulence Structure', *Boundary-Layer Meteorol.* **35**, 21–52.

Reid, J. D.: 1979, 'Markov Chain Simulations of Vertical Dispersion in the Neutral Surface Layer for Surface and Elevated Releases', *Boundary-Layer Meteorol.* **16**, 3–22.

Sawford, B. L and Guest, F. M.: 1987, 'Lagrangian Stochastic Analysis of Flux Gradient Relationships in the Convective Boundary Layer', *J. Atmos. Sci.* **44**, 1152–1165.

Sawford, B. L and Guest, F. M.: 1988, 'Uniqueness and Universality of Lagrangian Stochastic Models of Turbulent Dispersion', *Proceedings of the AMS 8th Symposium on Turbulence and Diffusion*, 25–29 April, San Diego, pp. 96–99.

Spiegel, M. R.: 1963, *Theory and Problems of Advanced Calculus*, McGraw-Hill Book Co., New York 384 pp.

Tavoularis, S. and Corrsin, S.: 1981, 'Experiments in Nearly Homogeneous Turbulent Shear Flow with a Uniform Mean Temperature Gradient. Part 1', *J. Fluid Mech.* **104**, 311–347.

Thompson, R.: 1971, 'Numeric Calculation of Turbulent Diffusion', *Quart. J. R. Meteorol. Soc.* **97**, 93–98.

Thomson, D. J.: 1984, 'Random Walk Modelling of Diffusion in Inhomogeneous Turbulence', *Quart. J. R. Meteorol. Soc.* **110**, 1107–1120.

Thomson, D. J.: 1987, 'Criteria for the Selection of Stochastic Models of Particle Trajectories in Turbulent Flows', *J. Fluid Mech.* **180**, 529–556.

van Dop, H., Nieuwstadt, F. T. M. and Hunt, J. C. R.: 1985, 'Random Walk Models for Particle Displacements in Inhomogeneous Unsteady Turbulent Flows', *Phys. Fluids* **28**, 1639–1653.

Weil, J. C.: 1990, 'A Diagnosis of the Asymmetry in Top-down and Bottom-up Diffusion using a Lagrangian Stochastic Model', *J. Atmos. Sci.* **47**, 501–515.

Wilson, J. D., Thurtell, G. W. and Kidd, G. E.: 1981, 'Numerical Simulation of Particle Trajectories in Inhomogeneous Turbulence-II. Systems with Variable Turbulent Velocity Scale', *Boundary-Layer Meteorol.* **21**, 423–441.